3898 *J. Phys. Chem. A* **1998,** *102,* 3898−3906

Synthesis and Spectroscopic and Electrochemical Characterization of Di- and Tetrasubstituted C_{60} Derivatives

Karl M. Kadish,*,[†] Xiang Gao,[†] Eric Van Caemelbecke,[†] Takeomi Hirasaka,[‡] Tomoyoshi Suenobu,[‡] and Shunichi Fukuzumi*,[‡]

University of Houston, Department of Chemistry, Houston, Texas 77204-5641 and Department of Applied Chemistry, Faculty of Engineering, Osaka University, Suita, Osaka 565, Japan

Received: February 11, 1998; In Final Form: March 24, 1998

The synthesis and electrochemical and spectroscopic characterization of fullerene derivatives of the type R_2C_{60} where R = $C_6H_5CH_2$, 2-$BrC_6H_4CH_2$, 3-$BrC_6H_4CH_2$, or 4-$BrC_6H_4CH_2$ and R_4C_{60} where R = $C_6H_5CH_2$ are reported. The first step in the synthesis involves an electron transfer between C_{60}^{2-} and RBr, and a similar initial electron-transfer step occurs between $[(C_6H_5CH_2)_2C_{60}]^{2-}$ and $C_6H_5CH_2Br$ during the synthesis of $(C_6H_5CH_2)_4C_{60}$. On the basis of NMR and UV−visible data, the investigated R_2C_{60} derivatives are identified as 1,4-adducts of C_{60}, whereas the isolated isomer of $(C_6H_5CH_2)_4C_{60}$ is characterized as possessing C_1 symmetry with the four benzyl groups being close to each other. The electrochemistry of each synthesized compound was determined in benzonitrile containing 0.1 M tetra-*n*-butylammonium perchlorate and each mono- and dianion of R_2C_{60} and R_4C_{60} were characterized by near-infrared spectroscopy. The near-infrared spectra of each species show two major "marker bands" which can be considered to be diagnostic of the fullerene derivative oxidation state.

Introduction

Electrochemistry has played a significant role in the early studies of C_{60} [1−5] since the method for preparation of fullerenes in macroscopic amounts was developed.[6] The discovery that C_{60} can reversibly accept multiple electrons in solution, as demonstrated by cyclic voltammetry,[1−5] has indicated that C_{60} is electron deficient and can act as an electrophile. This led to follow-up studies on the reactions of C_{60} with various nucleophiles,[7−10] which opened up ways for the derivatization of C_{60}. The dianion of C_{60} is very stable in solutions such as benzonitrile so that it is possible to generate C_{60}^{2-} electrochemically[11] or chemically[12,13] and use it as a starting material for the functionalization of C_{60}. Several groups have shown that the electrosynthesis of C_{60} derivatives from C_{60}^{2-} is a very efficient method.[11,14,15]

The derivatives of C_{60} have been speculated to possess some novel properties since C_{60} can be derivatized in three dimensions.[16−18] One important issue in derivatizing C_{60} is to understand how the electrochemical behavior of C_{60} is affected by the nature, number, and position of the addends.

There are numerous reports dealing with the electrochemistry of C_{60} derivatives.[19−32] In many cases, the first, second, and third reductions of C_{60} derivatives are shifted negatively by about 100−150 mV with respect to the first, second and third reductions of C_{60}, but there are little or no shifts in $E_{1/2}$ which can be ascribed to a substituent effect of the addend.[19−27] Sometimes, a good correlation between the $E_{1/2}$ values for reduction and the lowest unoccupied molecular orbital (LUMO) or LUMO + 1 of the compounds is observed.[28,29] Through-space orbital interactions or "periconjugation" has also been proposed to explain the electrochemical behavior of the spiromethanofullerenes and $(CN)_2C_{61}$.[30,31] A recent report on the electrochemistry of the dumbbell-shaped C_{120} shows that the dimer of C_{60} is reduced at an $E_{1/2}$ which is similar to that of C_{60}.[32]

The mono- and dianions of C_{60} are known to display characteristic absorption bands in the near-IR region.[33−41] Experimental and semiempirical work has indicated that the near-IR absorptions of C_{60} originate from the LUMO of C_{60}[34] but less is known about the mono- and dianionic forms of R_2C_{60},[21,33] and no spectroscopic data are available on $[R_4C_{60}]^{n-}$ where $n = 1$ or 2.

Only a few compounds of the type R_4C_{60} have been synthesized to date,[42−44] and it was therefore of interest to examine whether such compounds could be generated starting from R_2C_{60} where R is an alkyl or aryl group. The present paper reports the first electrogeneration of R_4C_{60} using R_2C_{60} as a starting material (R = $C_6H_5CH_2$) and the first electrochemistry of an R_4C_{60} derivative for comparison with that of R_2C_{60}. The data provide evidence for a complete loss of degeneracy of the LUMO in the investigated R_4C_{60} compound. The near-IR spectra of $[R_2C_{60}]^{n-}$ and $[R_4C_{60}]^{n-}$ where $n = 1$ or 2 are also reported in the paper, and for the first time, two characteristic absorption bands are reported for each anionic species. This result is related to a splitting of the t_{1u} and t_{1g} orbitals of C_{60} due to the decrease of symmetry.

Experimental Section

Chemicals. C_{60} (99.5%) was purchased from SES Research (Houston, TX) and used without further purification. Electrochemical grade tetra-*n*-butylammonium perchlorate (TBAP), purchased from Fluka, was recrystallized from absolute ethanol and dried in a vacuum at 313 K prior to use. Benzonitrile (PhCN) was distilled over P_2O_5 under vacuum at 305 K prior to use. $C_6H_5CH_2Br$ (98%), 2-$BrC_6H_4CH_2Br$ (98%), 3-BrC_6H_4-

---

* To whom correspondence should be addressed.

[†] University of Houston.

[‡] Osaka University.

S1089-5639(98)01060-3 CCC: $15.00

CH_2Br (99%), 4-$BrC_6H_4CH_2Br$ (98%), and TMS (99.9+%) were purchased from Aldrich and used as received. CS_2, hexanes, toluene, acetonitrile, methanol, and silica gel from EM Science (Gibbstown, NJ) were used without further treatment. $CDCl_3$ and CD_2Cl_2 for NMR measurements were purchased from Cambridge Isotope Laboratories (Andover, MA) and used as received.

Instrumentation. ^1H NMR spectra were recorded on either a Bruker AMX-600 or a General Electric QE-300 spectrometer in $CDCl_3/CS_2$, $CDCl_3$, or CD_2Cl_2 and referenced to TMS. UV−visible spectra of neutral R_2C_{60} and R_4C_{60} were recorded immediately after purification on the silica gel column with a Hewlett-Packard model 8453 diode array spectrophotometer. Near-IR spectra were obtained with both a Hewlett-Packard model 8453 diode array and a Perkin Elmer model 330 spectrophotometer. Cyclic voltammetry (CV) and controlled-potential bulk electrolyses were carried out using an EG & G Princeton Applied Research (PAR) 263 potentiostat/galvanostat. A conventional three-electrode cell was used for CV measurements and consisted of a glassy carbon working electrode, a platinum counter electrode, and a saturated calomel reference electrode (SCE). The SCE was separated from the bulk of the solution by a fritted glass bridge of low porosity which contained the solvent/supporting electrolyte mixture. Controlled-potential bulk electrolyses were performed in a glovebox from Vacuum Atmospheres Co. (Hawthorne, CA) using an "H" type cell which consisted of two platinum gauze electrodes (working and counter electrodes) separated by a sintered glass frit. Solutions containing about 2×10^{-4} M of the desired R_2C_{60} or R_4C_{60} anionic species were obtained by setting the applied potential at values 150 to 250 mV more negative than the $E_{1/2}$ of the $[R_xC_{60}]^{n-}/[R_xC_{60}]^{(n+1)-}$ redox couple (where $x = 2$ or 4) in the given solvent/supporting electrolyte system. CV measurements were carried out in the glovebox immediately after bulk electrolysis. The electrogenerated anions and dianions of R_2C_{60} and R_4C_{60} were then transferred from the bulk cell to a 1-cm quartz cuvette and the cuvettes removed from the glovebox after being capped with a rubber septum and sealed with Parafilm. Near-IR measurements of the electrogenerated anions were carried out under an N_2 atmosphere.

MALDI (matrix assisted laser desorption ionization) mass spectra were acquired at the UT-Houston Medical School, using a Perseptive Voyager Elite time-of-flight mass spectrometer equipped with delayed extraction and a nitrogen laser. The sample was dissolved in toluene or carbon disulfide. A saturated solution of 2,5-dihydroxybenzoic acid in 0.1% trifluoroacetic acid was used as a matrix. A solution containing 0.5 μL of matrix and 0.5 μL of sample was placed on the target. The sample was allowed to dry at room temperature and was protected from light.

Purification of $(C_6H_5CH_2)_4C_{60}$ by high-performance liquid chromatography (HPLC) was performed using a preparatory "Buckyclutcher I" column (Regis, Morton Grove, IL) with a 55:45 v/v mixture of hexanes/toluene as eluent and a flow rate of 8 mL/min. The eluted fractions were monitored by a UV−visible detector set at $\lambda = 365$ nm.

Synthesis of R_2C_{60}. To 80 mL of PhCN containing 0.2 M TBAP was added 200 mg of C_{60} after which $C_{60}{}^{2-}$ was generated by exhaustive electrolysis of the solution at −1.1 V vs SCE under a nitrogen atmosphere. The potentiostat was switched off, and while the solution was being stirred, a 10−50-fold excess of RBr ($R = C_6H_5CH_2$, 2-$BrC_6H_4CH_2$, 3-BrC_6H_4-CH_2, and 4-$BrC_6H_4CH_2$) was added under nitrogen all at once to the solution. This led to an immediate color change from red to green. The solution was stirred for 20 min during which time the color changed from green to dark brown. The mixture was dried with a rotary evaporator, and the residue was washed with acetonitrile to remove TBAP and excess RBr. The resulting product was first dissolved in neat CS_2 and then purified on a silica gel column using hexanes as eluent. Each R_2C_{60} derivative was recovered in ca. 50% yield. About 5% of unreacted C_{60} was also recovered after synthesis of each compound. There was also some red-colored material left on the top of the column, part of which could be eluted with toluene. However, the nature of the toluene fraction is unknown at the present time.

$(C_6H_5CH_2)_2C_{60}$: UV−visible (hexanes) λ_{max} [nm](ϵ) = 209 (1.7×10^5), 256 (1.2×10^5), 328 (3×10^4), 445 (7×10^3); ^1H NMR ($CDCl_3/CS_2$, 295 K, 600 MHz) $\delta = 7.51$ (d, $J = 7.3$ Hz, 2H), 7.41 (t, $J = 7.5$ Hz, 2H), 7.30 (t, $J = 7.5$ Hz, 1H), 3.75 (d, $J = 12.6$ Hz, 1H, H_a of CH_2), 3.71 (d, $J = 12.6$ Hz, 1H, H_b of CH_2); ^{13}C NMR ($CDCl_3/CS_2$, 295 K, 150 MHz) $\delta = 157.6$ (2C), 151.5 (2C),148.4 (2C), 147.0 (2C), 146.7 (5C),145.9 (2C), 145.3 (2C), 144.9 (2C), 144.6 (1C), 144.5 (2C), 144.2 (2C), 144.1 (4C), 143.9 (2C), 143.8 (2C), 143.5 (2C), 143.0 (2C), 142.9 (6C), 142.8 (4C), 142.5 (2C),142.4 (1C), 142.3 (2C), 141.9 (2C), 140.4 (1C), 138.6 (2C), 137.7 (2C), 136.0 (2C, Ph),130.9 (4C, Ph), 128.4 (4C, Ph), 127.4 (2C, Ph), 60.3 (2C), 48.5 (2C, CH_2).

$(2\text{-}BrC_6H_4CH_2)_2C_{60}$: UV−visible (hexanes) λ_{max} [nm](ϵ) = 209 (2.4×10^5), 256 (1.4×10^5), 328 (4×10^4), 445 (9×10^3); ^1H NMR ($CDCl_3/CS_2$, 295 K, 600 MHz) $\delta = 7.67$ (d, $J = 7.7$ Hz, 1H), 7.64 (d, $J = 7.9$ Hz, 1H), 7.42 (t, $J = 7.5$ Hz, 1H), 7.19 (t, $J = 7.5$ Hz, 1H), 4.16 (d, $J = 13.0$ Hz, 1H, H_a of CH_2), 3.94 (d, $J = 13.1$ Hz, 1H, H_b of CH_2); ^{13}C NMR ($CDCl_3/CS_2$, 295 K, 150 MHz) $\delta = 156.8$ (2C), 151.3 (2C), 148.6 (2C), 148.3 (2C), 147.1 (2C), 146.9 (5C), 145.8 (2C), 145.4 (2C), 145.0 (2C), 144.7 (3C), 144.6 (2C), 144.3 (2C), 144.2 (4C), 144.0 (2C), 143.9 (2C), 143.5 (2C), 143.1 (2C), 143.0 (4C), 142.9 (2C), 142.6 (2C), 142.4 (2C), 141.7 (1C), 141.8 (2C), 140.6 (1C), 138.7 (2C), 137.9 (2C), 135.9 (2C, Ph), 133.6 (2C, Ph), 133.0 (2C, Ph), 129.2 (2C, Ph), 127.4 (2C, Ph), 126.5 (2C, Ph), 59.6 (2C), 47.3 (2C, CH_2).

$(3\text{-}BrC_6H_4CH_2)_2C_{60}$: UV−visible (hexanes) λ_{max} [nm](ϵ) = 209 (2.0×10^5), 256 (1.3×10^5), 328 (4×10^4), 445 (9×10^3); ^1H NMR ($CDCl_3/CS_2$, 295 K, 600 MHz) $\delta = 7.67$ (s, 1H), 7.47 (t, $J = 9.2$ Hz, 2H), 7.33 (t, $J = 7.5$ Hz, 1H), 3.75 (d, $J = 13.0$ Hz, 1H, H_a of CH_2), 3.68(d, $J = 13.1$ Hz, 1H, H_b of CH_2); ^{13}C NMR ($CDCl_3/CS_2$, 295 K, 150 MHz) $\delta = 157.1$ (2C), 151.1 (2C), 148.6 (2C), 148.3 (2C), 147.2 (2C), 146.9 (4C), 146.5 (2C), 145.7 (2C), 145.5 (2C), 145.1 (2C), 144.7 (1C), 144.6 (2C), 144.3 (3C), 144.2 (4C), 144.1 (2C), 144.0 (2C), 143.6 (2C), 143.2 (2C), 143.0 (6C), 142.6 (2C), 142.4 (2C), 142.1 (2C), 141.9 (1C), 140.7 (1C), 138.7 (2C), 138.4 (2C, Ph), 137.7 (2C), 133.9 (2C, Ph), 130.8 (2C, Ph), 130.0 (2C, Ph), 129.6 (2C, Ph), 123.0 (2C, Ph), 59.9 (2C), 48.1 (2C, CH_2).

$(4\text{-}BrC_6H_4CH_2)_2C_{60}$: UV−visible (hexanes) λ_{max} [nm](ϵ) = 209 (2.0×10^5), 256 (1.3×10^5), 328 (4×10^4), 445 (7×10^3); ^1H NMR ($CDCl_3/CS_2$, 295 K, 600 MHz) $\delta = 7.55$ (d, $J = 8.2$ Hz, 2H), 7.42 (d, $J = 8.1$ Hz, 2H), 3.84 (d, $J = 13.1$ Hz, 1H, H_a of CH_2), 3.82 (d, $J = 13.1$ Hz, 1H, H_b of CH_2); ^{13}C NMR ($CDCl_3/CS_2$, 295 K, 150 MHz) $\delta = 156.8$ (2C), 151.1 (2C), 148.5 (2C), 148.2 (2C), 147.1 (2C), 146.8 (4C), 146.5 (2C), 145.7 (2C), 145.4 (2C), 144.9 (2C), 144.5 (1C), 144.4 (2C), 144.2 (3C), 144.1 (4C), 143.9 (4C), 143.5 (2C), 143.1 (2C), 142.9 (6C), 142.5 (2C), 142.2 (2C), 141.9 (2C), 141.8 (1C), 140.6 (1C), 138.7 (2C), 137.8 (2C), 134.8 (2C, Ph), 132.4 (4C, Ph), 131.5 (4C, Ph), 121.9 (2C, Ph), 59.8 (2C), 48.1 (2C, CH_2).

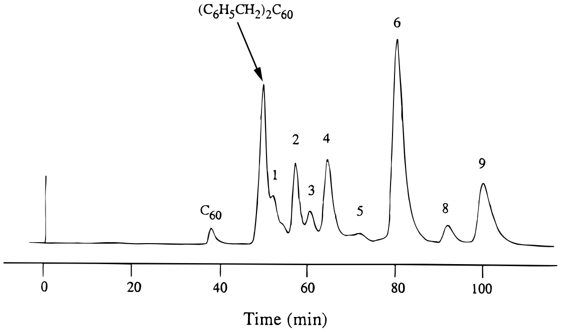

Figure 1. HPLC trace of the crude $[(C_6H_5CH_2)_2C_{60}]^{2-}/C_6H_5CH_2Br$ reaction product (after 60 min of reaction time between $[(C_6H_5CH_2)_2C_{60}]^{2-}$ and $C_6H_5CH_2Br$, see text).

Synthesis of $(C_6H_5CH_2)_4C_{60}$. The method described above for the synthesis of $(C_6H_5CH_2)_2C_{60}$ from C_{60} was applied to generate $(C_6H_5CH_2)_4C_{60}$ from $(C_6H_5CH_2)_2C_{60}$. The key point of this method is a chemical[12] or electrochemical[11] generation of the fullerene or substituted fullerene dianion which is then allowed to react with the alkyl halide to give R_2C_{60} or R_4C_{60}. In the present study, the dianion of $(C_6H_5CH_2)_2C_{60}$ was generated electrochemically in PhCN, 0.2 M TBAP at an applied potential of −1.15 V vs SCE. The reaction between $(C_6H_5CH_2)_2C_{60}$ and $C_6H_5CH_2Br$ was allowed to proceed for either 20 or 60 min. Benzonitrile, from the solution in the bulk cell, was removed by a rotary evaporator, after which the solid residue was washed with methanol and filtered to eliminate the TBAP supporting electrolyte and excess $C_6H_5CH_2Br$. The crude solid was mixed with a hexane/toluene mixture (55:45 v/v) and was analyzed by HPLC. Some material could not be eluted with the hexane/toluene mixture and required pure toluene to be eluted. Only the fraction eluted with the hexane/toluene mixture was analyzed.

The HPLC trace of the crude product (obtained after the reaction between $[(C_6H_5CH_2)_2C_{60}]^{2-}$ and $C_6H_5CH_2Br$ was allowed to proceed for 60 min) is shown in Figure 1. The most abundant fraction of the products (labeled as peak no. 6 in Figure 1) was isolated in pure form and is characterized as $(C_6H_5CH_2)_4C_{60}$.

$(C_6H_5CH_2)_4C_{60}$: UV−visible (hexanes) λ_{max} [nm]: 207, 247; ^{13}C NMR ($CDCl_3$, 295 K, 150 MHz) δ = 161.1 (1C), 156.6 (1C), 156.3 (1C), 154.8 (1C), 152.7 (1C), 151.8 (1C), 150.3 (1C), 149.9 (1C), 149.5 (1C), 149.0 (1C), 148.6 (1C), 148.2 (1C), 148.0 (1C), 148.0 (1C), 147.8 (3C), 147.6 (1C), 147.5 (1C), 147.4 (1C), 147.3 (1C), 147.1 (1C), 146.9 (1C),146.5 (1C), 146.3 (1C), 146.1 (1C), 146.0 (1C), 145.8 (1C), 145.8 (1C), 145.6 (1C), 145.5 (1C), 145.4 (1C), 145.3 (1C), 144.9 (1C), 144.7 (1C), 144.6 (1C), 144.5 (1C), 144.4 (1C), 144.2 (1C), 144.0 (1C), 143.8 (1C), 143.7 (1C), 143.5 (1C), 143.2 (1C), 143.1 (1C), 142.9 (1C), 142.8 (1C), 142.8 (2C), 142.6 (2C), 142.5 (1C), 139.8 (1C), 139.6 (1C), 138.2 (1C), 137.3 (1C), 136.5 (1C, Ph), 136.4 (1C, Ph), 136.2 (1C, Ph), 135.8 (1C, Ph), 131.2 (2C, Ph), 131.0 (2C, Ph), 131.0 (2C, Ph), 130.7 (2C, Ph), 128.8 (2C, Ph), 128.5 (2C, Ph), 128.3 (2C, Ph), 127.9 (1C, Ph), 127.8 (2C, Ph), 127.5 (1C, Ph), 127.2 (1C, Ph), 126.8 (1C, Ph), 61.4 (1C), 58.6 (2C), 57.1 (1C), 47.5 (1C, CH_2), 47.4 (1C, CH_2), 46.9 (1C, CH_2), 45.7 (1C, CH_2).

Kinetic Measurements. $[(C_6H_5CH_2)_2C_{60}]^{2-}$, for kinetic measurements, was produced by reduction of $(C_6H_5CH_2)_2C_{60}$ by using naphthalene radical anion as a reducing agent. Typically, an appropriate aliquot of a THF solution of naphthalene radical anion (1.0×10^{-4} to 2.0×10^{-3} M) was added to a quartz cuvette (10 mm i.d.) which contained a deaerated PhCN solution (3.0 cm^3) of $(C_6H_5CH_2)_2C_{60}$ (2.8×10^{-4} M) to produce $[(C_6H_5CH_2)_2C_{60}]^{2-}$. When $C_6H_5CH_2Br$ was added to the $[(C_6H_5CH_2)_2C_{60}]^{2-}$ solution, the absorption band at λ_{max} = 903 nm due to $[(C_6H_5CH_2)_2C_{60}]^{2-}$ disappeared. The visible−near-IR spectra were recorded on a Hewlett-Packard 8452A or 8453 diode array spectrophotometer which was thermostated at 298 K. The rate constant for reaction of $[(C_6H_5CH_2)_2C_{60}]^{2-}$ with $C_6H_5CH_2Br$ and other alkyl halides in deaerated PhCN at 298 K was determined by following a decrease in absorbance due to $[(C_6H_5CH_2)_2C_{60}]^{2-}$ (λ = 903 nm) under pseudo-first-order conditions where the concentration of RX was maintained at >10-fold excess of the $[(C_6H_5CH_2)_2C_{60}]^{2-}$ concentration (2.8×10^{-4} M). Pseudo-first-order rate constants were determined by a least-squares curve fit using a Macintosh personal computer. The pseudo-first-order plots were linear for three or more half-lives with correlation coefficients greater than 0.999.

Theoretical Calculations. Theoretical calculations were performed using the MOPAC program (version 6) which is incorporated in the MOLMOLIS program by Daikin Industries, Ltd. The PM3 Hamiltonian was used for the semiempirical MO calculations.[45] Final geometries and energetics were obtained by optimizing the total molecular energy with respect to all structural variables.

Results and Discussion

Synthesis and Spectroscopic Characterization of R_2C_{60}. The synthesis of each $(x\text{-}BrC_6H_4CH_2)_2C_{60}$ derivative (x = 2, 3, or 4) examined in this study is proposed to occur via a mechanism similar to that reported for $(C_6H_5CH_2)_2C_{60}$.[12] The first step should involve an electron transfer between electrogenerated $C_{60}{}^{2-}$ and x-$BrC_6H_4CH_2Br$, followed by a fast radical coupling and further reaction of the product with another molecule of x-$BrC_6H_4CH_2Br$ via nucleophilic substitution.

The crystal structure of $(C_6H_5CH_2)_2C_{60}$ shows the compound to be a 1,4-adduct of C_{60}.[12] The UV−visible spectra of R_2C_{60} (R = 2-$BrC_6H_4CH_2$, 3-$BrC_6H_4CH_2$, or 4-$BrC_6H_4CH_2$) in hexanes show a pattern similar to that of $C_{60}(C_6H_5CH_2)_2$ in that four absorption bands are seen at about 209, 256, 328, and 445 nm, thus suggesting that each investigated compound is also a 1,4-adduct of C_{60}. The visible band located at 445 nm has not been observed for C_{60}[46,47] or any known 1,2-R_2C_{60} derivative[48] and may well be a diagnostic criterion for the generation of 1,4-adducts of C_{60}.[49−51]

^1H NMR Spectra. The ^1H NMR spectra of each R_2C_{60} derivative in $CDCl_3$ are illustrated in Figure 2. All four compounds show an AB quartet between 3.68 and 4.16 ppm which results from the CH_2 groups of the benzyl groups. Each compound also exhibits peaks due to aromatic protons in the range 7.1−7.7 ppm, and this is consistent with the proposed structure.

In a 1,2-disubstituted C_{60} derivative, the three carbons C1, C2 and C3 bonded to the sp^3 carbon C3′ are not all different, i.e., C1 and C2 are equivalent (see Figure 3a), so that the two sp^3 carbons C3′ and C3 to which the substituents are attached are not chiral centers. For such a configuration of the substituents, the two methylene protons of the benzyl groups are equivalent[52,53] and give only a single resonance as is the case for $(C_6H_5CH_2)HC_{60}$.[13] In contrast, the neighboring carbons of each sp^3 carbon of the C_{60} cage in the 1,4-disubstituted C_{60} derivative (Figure 3b) are not equivalent, and consequently, these two sp^3 carbons are chiral centers. In such a configuration of the substituents, the methylene protons of the benzyl groups are diastereotopic and give an AB quartet.[52,53] AB quartets are

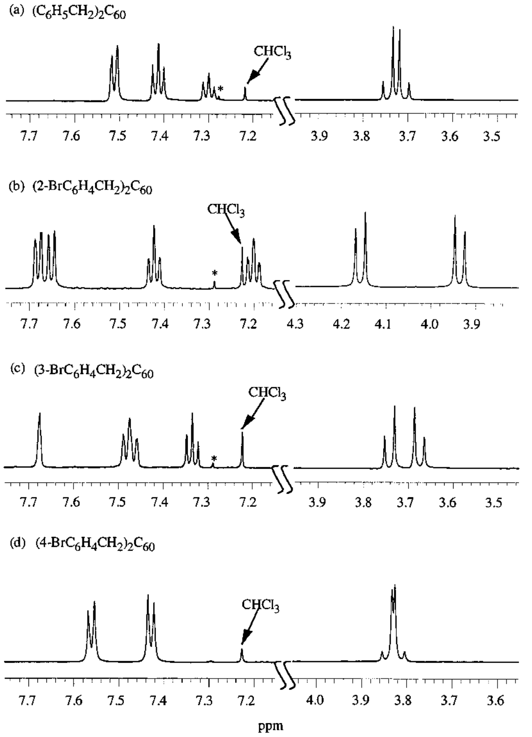

Figure 2. ^1H NMR of R_2C_{60} in $CS_2/CDCl_3$, where R = (a) $C_6H_5CH_2$, (b) $2\text{-}BrC_6H_4CH_2$, (c) $3\text{-}BrC_6H_4CH_2$ and (d) $4\text{-}BrC_6H_4CH_2$. The peak marked with an asterisk is due to an unknown impurity in CS_2.

observed for all of the R_2C_{60} derivatives investigated in the present study, thus implying that each compound is a 1,4-addition product of C_{60}.

Chemical shifts of the methylene protons in the investigated R_2C_{60} derivatives are listed in Table 1. The two methylene proton resonances of $(2\text{-}BrC_6H_4CH_2)_2C_{60}$ are shifted about 0.41 (H_a) and 0.23 (H_b) ppm downfield with respect to the two resonances of $(C_6H_5CH_2)_2C_{60}$, while the methylene proton resonances of $(3\text{-}BrC_6H_4CH_2)_2C_{60}$ and $(4\text{-}BrC_6H_4CH_2)_2C_{60}$ have chemical shifts similar to those of $(C_6H_5CH_2)_2C_{60}$. The large difference for the 2-Br derivative might be due in part to a substituent effect of the Br group on the phenyl ring, but literature data for toluene and Br-substituted toluene show no substituent effect on chemical shifts of the methyl protons,[54] thus suggesting the lack of a substituent effect on the proton resonances for compounds in the $(x\text{-}BrC_6H_4CH_2)_2C_{60}$ series. On the other hand, the $(2\text{-}BrC_6H_4CH_2)_2C_{60}$ complex is clearly different from the other two $(x\text{-}BrC_6H_4CH_2)_2C_{60}$ derivatives, both in the absolute value of the chemical shifts and in the value of $\Delta\delta$. This latter value (expressed in ppm) describes the magnitude of separation between the two doublets of the AB quartet, when measured from the centers of the doublets.

Studies by Whitesides et al.[55,56] have shown that the conformation of a phenyl ring with respect to the methylene protons of a benzyl group has a significant effect on $\Delta\delta$. The authors have demonstrated that the value of $\Delta\delta$ will be small when the two conformations in Chart 1 are equally populated or when a conformation analogous to that in Chart 1b is favored. It is thus reasonable to believe that the value of $\Delta\delta$ will be large when a conformation analogous to that shown in Chart 1a is favored. The $\Delta\delta$ value of $(2\text{-}BrC_6H_4CH_2)_2C_{60}$ is significantly larger than that of the other three investigated compounds, and this result could be related to a hindered rotation of the phenyl group[57] on the basis of analogy with the studies by Whitesides et al.[55,56]

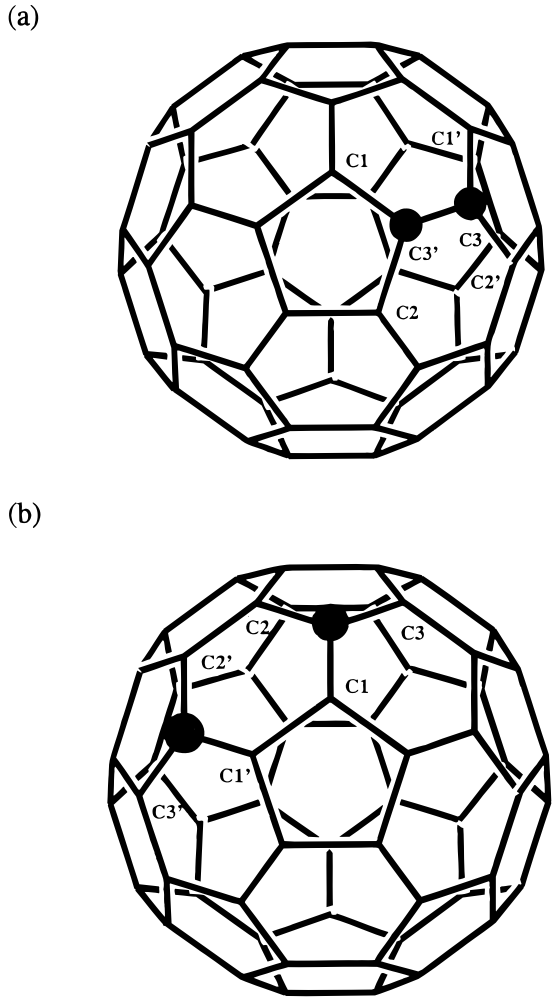

Figure 3. (a) Diagram for a 1,2-disubstituted compound. Due to a symmetry plane along the two sp^3 carbons of C_{60}, C1 is equivalent to C2 and C1′ is equivalent to C2′. (b) Diagram for a 1,4-disubstituted compound. C1, C2, and C3 are nonequivalent, and this is also the case for C1′, C2′, and C3′ due to the lack of a symmetry plane along the two sp^3 carbons of C_{60}. Black circles indicate the position of the substituents.

TABLE 1: ^{1}H NMR Resonances for the Methylene Protons of $C_{60}(R)_2$ in $CS_2/CDCl_3$

	δ, chemical shift (ppm)		coupling constant (Hz)		
compound	H_a	H_b	J_1	J_2	Δδ (ppm)[a]
$(C_6H_5CH_2)_2C_{60}$	3.75	3.71	12.6	12.6	0.04
$(2\text{-}BrC_6H_4CH_2)_2C_{60}$	4.16	3.94	13.0	13.1	0.22
$(3\text{-}BrC_6H_4CH_2)_2C_{60}$	3.75	3.68	13.0	13.1	0.07
$(4\text{-}BrC_6H_4CH_2)_2C_{60}$	3.84	3.82	13.1	13.1	0.02

[a] Δδ is the separation between the centers of two doublets in ppm for an AB quartet.

^{13}C NMR Spectra. The ^{13}C NMR spectrum of each investigated R_2C_{60} derivative reveals two characteristic features. One is the presence of two peaks at about 49 and 60 ppm which correspond to the sp^3 carbons of CH_2 and C_{60}, respectively. The other is the presence of 25−26 peaks between 137 and 157 ppm which are assigned to the sp^2 carbons of C_{60}. This number of peaks is smaller than the 31 peaks theoretically expected for a 1,4-adduct of C_{60} with C_s symmetry due to the presence of several overlapping peaks.[48] However, the observed number of peaks is larger than the 16 which are calculated for a 1,2-adduct with C_{2v} symmetry,[48] thus indicating that the R_2C_{60} derivatives are best described as 1,4-addition products of C_{60}.

CHART 1

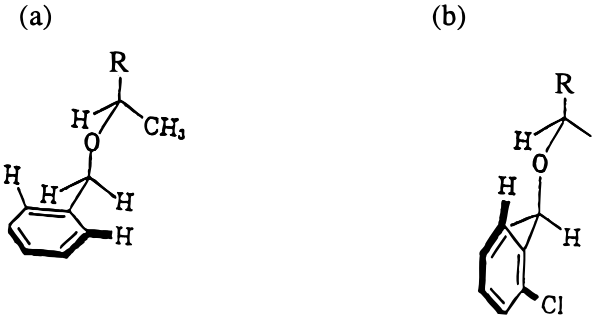

TABLE 2: Observed Second-order Rate Constants (k_{obs}) for the Reactions of $[(C_6H_5CH_2)_2C_{60}]^{2-}$, C_{60}^{2-}, and $[(CH_3)_4Q^{\bullet}]^-$ with Various Alkyl Halides (R*X*) in Deaerated PhCN at 298 K

R*X*	k_{obs}-$[(C_6H_5CH_2)_2C_{60}]^{2-}$ [a] $M^{-1}\,s^{-1}$	$k_{obs}C_{60}^{2-}$ [a] $M^{-1}\,s^{-1}$	k_{obs}-$[(CH_3)_4Q^{\bullet}]^-$ [a] $M^{-1}\,s^{-1}$
t-C_4H_9I	6.2×10^{-2}	4.7×10^{-2}	2.6×10^{-1}
$(CH_3)_2C{=}CHCH_2Cl$	1.5×10^{-1}	5.1×10^{-2}	2.4×10^{-1}
$C_6H_5CH_2Br$	1.6×10	8.0×10^{-1}	1.8
$CH_2{=}CHCH_2Br$	1.1×10	2.2	1.5

[a] The experimental error is ± 5%.

The ^{13}C NMR spectrum of each investigated R_2C_{60} shows additional resonances between 120 and 139 ppm which are assigned to carbons of the phenyl rings.

The UV−visible, ^1H NMR, and ^{13}C NMR spectra of each compound are self-consistent and imply that the four investigated R_2C_{60} derivatives are best described as 1,4-adducts of C_{60}. A peak is found at $m/z = 1059$ in the mass spectra of both $(2\text{-}BrC_6H_4CH_2)_2C_{60}$ and $(3\text{-}BrC_6H_4CH_2)_2C_{60}$. This *m*/*z* ratio corresponds to the $[M + H]^+$ species of each derivative, thus confirming their formulation as R_2C_{60}.

Mechanism for Synthesis of $(C_6H_5CH_2)_4C_{60}$ from $(C_6H_5CH_2)_2C_{60}$. The reaction of C_{60}^{2-} with $C_6H_5CH_2Br$ occurs via an initial electron transfer from C_{60}^{2-} to $C_6H_5CH_2Br$[12], and the observed second-order rate constant agrees with the value expected for an electron transfer on the basis of the Marcus theory.[58] The nucleophilic reactivity of C_{60}^{2-} is very low because of the highly delocalized negative charge.[12] In the case of $[(C_6H_5CH_2)_2C_{60}]^{2-}$, however, the negative charge may be more localized than in the case of C_{60}^{2-}. To examine whether the reaction of $[(C_6H_5CH_2)_2C_{60}]^{2-}$ with $C_6H_5CH_2Br$ occurs via an initial electron transfer from $[(C_6H_5CH_2)_2C_{60}]^{2-}$ to $C_6H_5CH_2Br$ or via a nucleophilic attack of $[(C_6H_5CH_2)_2C_{60}]^{2-}$ on $C_6H_5CH_2Br$, the rate constants for reactions of $[(C_6H_5CH_2)_2C_{60}]^{2-}$ with $C_6H_5CH_2Br$ and other alkyl halides were determined and compared with rate constants expected for an electron-transfer reaction.

The rate constant for the reaction of $[(C_6H_5CH_2)_2C_{60}]^{2-}$ with $C_6H_5CH_2Br$ was determined by monitoring the disappearance of an absorption band due to $[(C_6H_5CH_2)_2C_{60}]^{2-}$ at 903 nm. The rate constant obeys pseudo-first-order kinetics under the present experimental conditions, where the $C_6H_5CH_2Br$ concentration is more than 10 times the $[(C_6H_5CH_2)_2C_{60}]^{2-}$ concentration. The pseudo-first-order rate constant is proportional to the $C_6H_5CH_2Br$ concentration, and a second-order rate constant (k_{obs}) is determined from the proportionality constant. The k_{obs} values for reaction of $[(C_6H_5CH_2)_2C_{60}]^{2-}$ with other alkyl halides were determined at 298 K in PhCN and are listed in Table 2 along with the corresponding k_{obs} for the reactions of C_{60}^{2-} with the same alkyl halides.

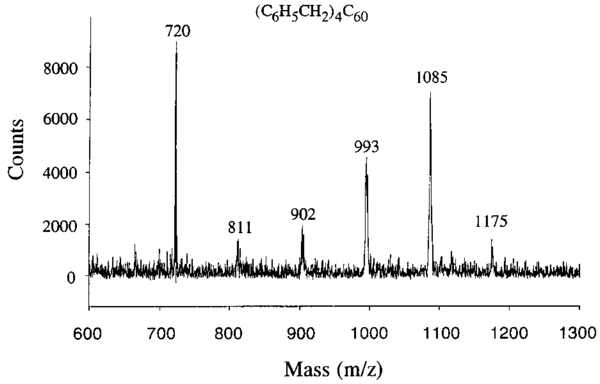

Figure 4. Mass spectrum of $(C_6H_5CH_2)_4C_{60}$.

TABLE 3: Theoretical *m*/*z* Values for Fragment Ions and Gas Phase Products of $(C_6H_5CH_2)_4C_{60}$

species	*m*/*z*
$[(C_6H_5CH_2)_4C_{60} + H]^+$	1085
$[(C_6H_5CH_2)_4C_{60} - C_6H_5CH_2]^+$	993
$[(C_6H_5CH_2)_4C_{60} - 2C_6H_5CH_2]^+$	902
$[(C_6H_5CH_2)_4C_{60} - 3C_6H_5CH_2]^+$	811
$[(C_6H_5CH_2)_4C_{60} - 4C_6H_5CH_2]^+$	720
$[(C_6H_5CH_2)_4C_{60} + C_6H_5CH_2]^+$	1175

Rate constants for the electron-transfer reactions of a tetramethylsemiquinone radical anion $[(CH_3)_4Q^{\bullet}]^-$ with alkyl halides were determined in PhCN at 298 K by following the decrease in absorbance of a band at 442 nm which is assigned to $[(CH_3)_4Q^{\bullet}]^-$. The k_{obs} values for these electron-transfer reactions are listed in Table 2 along with k_{obs} values for the reactions of C_{60}^{2-} and $[(C_6H_5CH_2)_2C_{60}]^{2-}$ with the same alkyl halides. The data agrees well with values for an electron-transfer reaction from $[(CH_3)_4Q^{\bullet}]^-$ to the alkyl halides (Table 2), supporting a previous conclusion that the reaction of C_{60}^{2-} with alkyl bromides occurs via a rate-determining electron-transfer step between C_{60}^{2-} and the alkyl bromide.[12] The k_{obs} values for the reaction of $[(C_6H_5CH_2)_2C_{60}]^{2-}$ with alkyl halides are always larger than values for reaction of C_{60}^{2-} with the same alkyl halides (see Table 2). The fact that the k_{obs} values for $[(C_6H_5CH_2)_2C_{60}]^{2-}$ are larger than those for C_{60}^{2-} is consistent with an electron-transfer mechanism since the oxidation potential of $[(C_6H_5CH_2)_2C_{60}]^{2-}$ is more negative than that of C_{60}^{2-}.[12]

The proposed mechanism also agrees with the reactivity between $[(C_6H_5CH_2)_2C_{60}]^{2-}$ and *t*-C_4H_9I, since a nucleophilic attack of $[(C_6H_5CH_2)_2C_{60}]^{2-}$ on the sterically bulky *t*-C_4H_9I would be unlikely to occur. Thus, an initial electron transfer from $[(C_6H_5CH_2)_2C_{60}]^{2-}$ to $C_6H_5CH_2Br$ may occur to give the $[(C_6H_5CH_2)_2C_{60}]^{\bullet-}/C_6H_5CH_2^{\bullet}$ radical pair which is produced by an instant cleavage of the C−Br bond upon the dissociative electron transfer to $C_6H_5CH_2Br$. The electron transfer would then be followed by a fast radical coupling between $[(C_6H_5CH_2)_2C_{60}]^{\bullet-}$ and $C_6H_5CH_2^{\bullet}$ to give $[(C_6H_5CH_2)_3C_{60}]^-$ which further reacts with another molecule of $C_6H_5CH_2Br$ to yield the final product, $(C_6H_5CH_2)_4C_{60}$.

Synthesis and Spectroscopic Characterization of $(C_6H_5CH_2)_4C_{60}$. The procedure for the synthesis of $(C_6H_5CH_2)_4C_{60}$ has been described in the Experimental Section. The mass spectrum of $(C_6H_5CH_2)_4C_{60}$ is shown in Figure 4, while the *m*/*z* ratios for the fragmentation and/or gas-phase reaction products are listed in Table 3.

The peak for the $[M + H]^+$ protonated molecular ion of $(C_6H_5CH_2)_4C_{60}$ occurs at $m/z = 1085$ and has about a 90% relative intensity with respect to that of C_{60} ($m/z = 720$), thus indicating that the tetra-adduct of C_{60} is quite stable under these

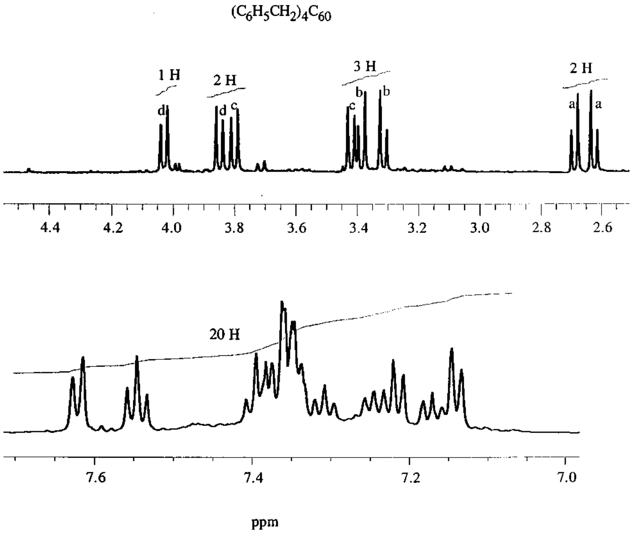

Figure 5. ^1H NMR spectrum of $(C_6H_5CH_2)_4C_{60}$ in CD_2Cl_2.

TABLE 4: ^1H NMR Resonances for the Methylene Protons of $(C_6H_5CH_2)_4C_{60}$ in CD_2Cl_2

AB quartet	δ, chemical shift (ppm) H_a	H_b	coupling constant (Hz) J_1	J_2	$\Delta\delta$ (ppm)[a]
I (aa)	2.69	2.62	13.2	13.2	0.07
II (bb)	3.39	3.31	13.2	13.2	0.08
III (cc)	3.80	3.42	13.2	13.2	0.38
IV (dd)	4.03	3.85	13.2	13.2	0.18

[a] $\Delta\delta$ is the separation between the centers of two doublets in ppm for an AB quartet.

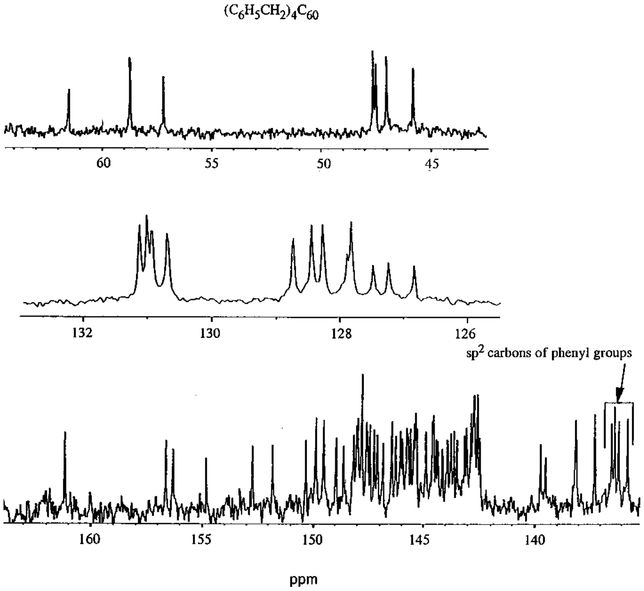

Figure 6. ^{13}C NMR spectra of $(C_6H_5CH_2)_4C_{60}$ in $CDCl_3$.

experimental conditions. The mass spectrum of $(C_6H_5CH_2)_4C_{60}$ shows four peaks at $m/z = 993$, 902, 811, and 720 which correspond to a successive loss of four $C_6H_5CH_2$ groups. There is also a peak at $m/z = 1175$ which is due to a reaction between $(C_6H_5CH_2)_4C_{60}$ and $C_6H_5CH_2^+$ in the gas phase. Indeed, under our experimental conditions, this peak would be located at $m/z = 1176$ rather than at 1175 if $(C_6H_5CH_2)_5C_{60}$ were initially present in the analyzed product.

The ^1H NMR spectrum of $(C_6H_5CH_2)_4C_{60}$ in CD_2Cl_2 is shown in Figure 5, while Table 4 lists resonances of the CH_2 groups. The spectrum of the compound shows four AB quartets between 2.62 and 4.03 ppm which are consistent with the presence of four CH_2 groups on the C_{60} skeleton. The spectrum of the compound in $CDCl_3$ is also consistent with the presence of four CH_2 groups on the molecule. It shows only seven doublets, but one has an integrated area twice that of the other six doublets. The AB quartets I (aa) and II (bb) of $(C_6H_5CH_2)_4C_{60}$ in CD_2Cl_2 exhibit very small $\Delta\delta$ values of 0.07−0.08 ppm (see Table 4). These values are similar in magnitude to the $\Delta\delta = 0.04$ ppm for the AB quartet of $(C_6H_5CH_2)_2C_{60}$ (see Table 4), thus indicating that two of the four phenyl rings of $(C_6H_5CH_2)_4C_{60}$ have relatively free rotation as is the case for the two phenyl rings of $(C_6H_5CH_2)_2C_{60}$. However, the AB quartets III (cc) and IV (dd) of $(C_6H_5CH_2)_4C_{60}$ have $\Delta\delta$ values of 0.38 and 0.18 ppm, respectively (Table 4). These values are much higher than those for the AB quartets I (aa) and II (bb) of the same compound but are similar in magnitude to the $\Delta\delta$ values of $(2\text{-}BrC_6H_4CH_2)_2C_{60}$, thus suggesting that these two benzyl groups are more favored to remain in a conformation similar to the conformation of the benzyl group shown in Chart 1a. This effect may be explained in terms of interaction between closely positioned benzyl groups.

The resonances corresponding to the benzyl group aromatic protons of $(C_6H_5CH_2)_4C_{60}$ are more spread out and lacking in symmetry as compared to those for the benzyl groups of $(C_6H_5CH_2)_2C_{60}$. This result agrees with NMR data for the methylene protons, indicating that the investigated $(C_6H_5CH_2)_4C_{60}$ isomer possesses C_1 symmetry.

The ^{13}C NMR spectrum of $(C_6H_5CH_2)_4C_{60}$ in $CDCl_3$ is shown in Figure 6. Peaks are seen at 45.7, 46.9, 47.4, and 47.5 ppm, and these can be assigned to the four inequivalent carbons of the CH_2 groups of $(C_6H_5CH_2)_4C_{60}$ since chemical shifts for the CH_2 carbons of R_2C_{60} where R = $C_6H_5CH_2$, $2\text{-}BrC_6H_4CH_2$, $3\text{-}BrC_6H_4CH_2$, or $4\text{-}BrC_6H_4CH_2$ range from 47.3 to 48.5 ppm. Signals for the sp^3 carbons of the C_{60} skeleton are observed between 56 and 62 ppm as is the case of R_2C_{60}, although only three out of the four expected signals can be seen due to an overlap in the resonances. The sp^2 carbon resonances of the four different benzene rings are seen between 126 and 137 ppm while a total of 52 peaks, which correspond to the sp^2 carbons of the C_{60} skeleton, are observed between 137 and 162 ppm. The ^{13}C NMR spectrum is therefore consistent with the presence of four inequivalent benzyl groups on the C_{60} skeleton and shows that the compound has a C_1 symmetry.

Cyclic Voltammetry. The cyclic voltammograms of C_{60}, $(C_6H_5CH_2)_2C_{60}$, and $(C_6H_5CH_2)_4C_{60}$ in PhCN, 0.1 M TBAP between 0.0 and −2.0 V vs SCE are shown in Figure 7, while the electrochemical data are summarized in Table 5. $(C_6H_5CH_2)_2C_{60}$ undergoes three reversible one-electron reductions at $E_{1/2} = -0.51$, -0.99, and -1.50 V vs SCE. The addition of two benzyl groups on the C_{60} cage causes the reduction potential to shift negatively.

Table 5 also lists the $E_{1/2}$ values for the reductions of the three Br-substituted benzyl C_{60} derivatives. Due to the electronic effect of the Br group, one would expect to see that all of the compounds containing Br atoms are easier to reduce than the unbrominated derivative. However, the first reduction potential of $(2\text{-}BrC_6H_4CH_2)_2C_{60}$ is identical to that of $(C_6H_5CH_2)_2C_{60}$, and the overall data in Table 5 indicate that there is no significant effect of the Br substitution on the electrochemistry of the investigated R_2C_{60} compounds.

$(C_6H_5CH_2)_4C_{60}$ undergoes reversible one-electron reductions at $E_{1/2} = -0.68$, -1.11, and -1.88 V vs SCE in PhCN, 0.1 M TBAP. The addition of two more benzyl groups onto the $(C_6H_5CH_2)_2C_{60}$ skeleton shifts cathodically each reduction of the compound, and this is similar to what is observed upon going

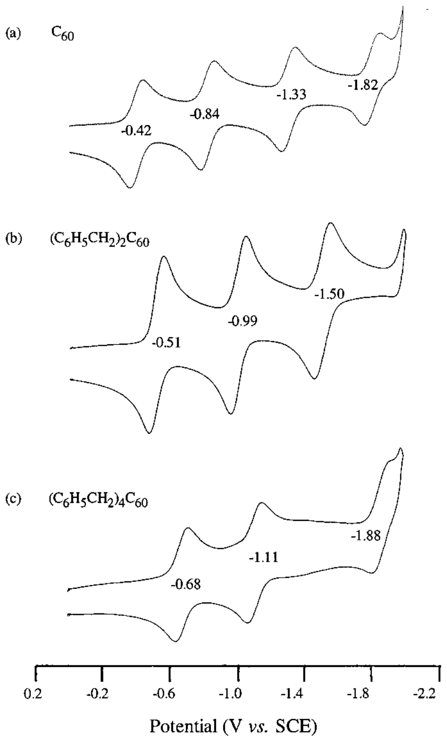

Figure 7. Cyclic voltammograms of (a) C_{60}, (b) $(C_6H_5CH_2)_2C_{60}$, and (c) $(C_6H_5CH_2)_4C_{60}$ in PhCN, 0.1 M TBAP.

TABLE 5: Reduction Potentials of C_{60}, R_2C_{60}, and R_4C_{60} in PhCN Containing 0.1 M TBAP

compound	$E_{1/2}$ (V vs SCE) first	second	third
C_{60}	−0.42	−0.84	−1.33
$(C_6H_5CH_2)_2C_{60}$	−0.51	−0.99	−1.50
$(2\text{-}BrC_6H_4CH_2)_2C_{60}$	−0.51	−0.96	−1.48
$(3\text{-}BrC_6H_4CH_2)_2C_{60}$	−0.47	−0.99	−1.48
$(4\text{-}BrC_6H_4CH_2)_2C_{60}$	−0.48	−1.00	−1.48
$(C_6H_5CH_2)_4C_{60}$	−0.68	−1.11	−1.88

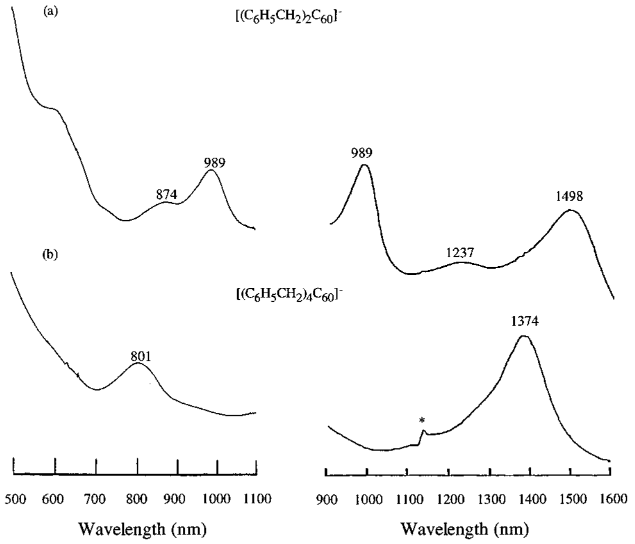

Figure 8. Near-IR spectra in PhCN, 0.2 M TBAP of (a) $[(C_6H_5CH_2)_2C_{60}]^-$ and (b) $[(C_6H_5CH_2)_4C_{60}]^-$. The peak marked with an asterisk is due to an artifact in the instrument.

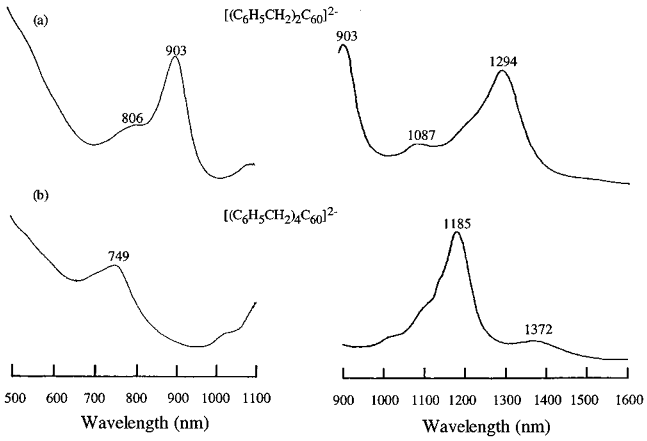

Figure 9. Near-IR spectra in PhCN, 0.2 M TBAP of (a) $[(C_6H_5CH_2)_2C_{60}]^{2-}$ and (b) $[(C_6H_5CH_2)_4C_{60}]^{2-}$.

from C_{60} to $(C_6H_5CH_2)_2C_{60}$. The first two reductions of $(C_6H_5CH_2)_4C_{60}$ are negatively shifted by 170 and 120 mV with respect to the first and second reductions of $(C_6H_5CH_2)_2C_{60}$, but a much larger negative shift of 380 mV is seen in the case of the third reduction This difference may be caused by a significant split in the degeneracy of the triply degenerate t_{1u} orbitals of C_{60} in R_4C_{60} which has no symmetry as compared to R_2C_{60}. Theoretical calculations of the molecular orbital levels of C_{60}, $(C_6H_5CH_2)_2C_{60}$, and $(C_6H_5CH_2)_4C_{60}$ show that the LUMOs which are triply degenerate in C_{60} (−2.89 eV) are split into two almost degenerate orbitals (−2.72 and −2.70 eV) and a higher orbital (−2.46 eV) in $(C_6H_5CH_2)_2C_{60}$ and further split into three separate orbitals (−2.56 eV, −2.47 eV, and −2.24 eV) in $(C_6H_5CH_2)_4C_{60}$.[59]

The oxidative behaviors of R_2C_{60} and R_4C_{60} complexes were also examined by cyclic voltammetry, but none of the compounds undergoes a reversible oxidation under our experimental conditions.

Near-IR Spectra. The near-IR spectra of $[(C_6H_5CH_2)_2C_{60}]^{n-}$ and $[(C_6H_5CH_2)_4C_{60}]^{n-}$ where $n = 1$ or 2 are shown in Figures 8 and 9, while Table 6 lists the major near-IR bands of the

TABLE 6. Spectral Data for Mono- and Dianions of C_{60}, $(R)_2C_{60}$ Where R = $C_6H_5CH_2$, $2\text{-}BrC_6H_4CH_2$, $3\text{-}BrC_6H_4CH_2$, or $4\text{-}BrC_6H_4CH_2$ and $(R)_4C_{60}$ Where R = $C_6H_5CH_2$ in PhCN Contaning 0.2 M TBAP[a]

	λ_{max} (nm) and ϵ (M^{-1} cm^{-1}) in parentheses					
	monoanion		dianion		ΔE (eV)[b]	
compound	band I	band II	band I	band II	band I	band II
C_{60}	1078 (12 000)[c]		952 (16 000)[c]		0.15	
$(C_6H_5CH_2)_2C_{60}$	989 (1 900)	1498 (1 500)	903 (5 200)	1294 (4 300)	0.12	0.13
$(2\text{-}BrC_6H_4CH_2)_2C_{60}$	988 (1 800)	1505 (1 300)	903 (5 800)	1300 (4 800)	0.12	0.13
$(3\text{-}BrC_6H_4CH_2)_2C_{60}$	992 (1 500)	1501 (900)	904 (6 100)	1300 (4 700)	0.12	0.13
$(4\text{-}BrC_6H_4CH_2)_2C_{60}$	994 (1 500)	1495 (900)	904 (5 800)	1299 (5 000)	0.12	0.13
$(C_6H_5CH_2)_4C_{60}$	801 (1 300)	1374 (1 700)	749 (2 800)	1185 (5 800)	0.11	0.14

[a] The average uncertainty in ϵ measurement is ca. 10%. [b] ΔE is the energy difference between the two bands of dianions and monoanions. [c] Values are taken from ref 34.

singly and doubly reduced forms of C_{60} and R_2C_{60} (R = $C_6H_5CH_2$, 2-$BrC_6H_4CH_2$, 3-$BrC_6H_4CH_2$, and 4-$BrC_6H_4CH_2$) and R_4C_{60} (R = $C_6H_5CH_2$).

The near-IR bands of C_{60}^- and C_{60}^{2-} are quite different from each other and are characteristic of the C_{60} anion oxidation state.[33-41] The measured peak maxima vary from 1064 to 1080 nm for the C_{60} monoanion and from 945 to 952 nm for the C_{60} dianion, depending upon the solution conditions. The near-IR spectrum of $[(C_6H_5CH_2)_2C_{60}]^-$ in PhCN, 0.2 M TBAP consists of two major bands at 989 and 1498 nm as well as two minor bands at 874 and 1237 nm. On the other hand, the major bands of $[(C_6H_5CH_2)_2C_{60}]^{2-}$ are located at 903 and 1294 nm while the minor bands appear at 806 and 1087 nm. As is the case for C_{60}, near-IR bands of the dianionic species, $[(C_6H_5CH_2)_2C_{60}]^{2-}$, are blue-shifted with respect to those of the monoanionic species, $[(C_6H_5CH_2)_2C_{60}]^-$. The mono- and dianions of (x-$BrC_6H_4CH_2)_2C_{60}$ (x = 2, 3 or 4) display absorptions similar to those of $(C_6H_5CH_2)_2C_{60}$, but the spectra differ slightly in shape upon going from one compound to another, and this could suggest an effect of the Br position on spectra of the R_2C_{60} mono- and dianions.

The spectrum of $[(C_6H_5CH_2)_4C_{60}]^-$ displays two major bands at 1374 and 801 nm (see Figure 8 and Table 6), while the doubly reduced species exhibits corresponding major bands at 1185 and 749 nm (see Figure 9 and Table 6). The spectrum of $[(C_6H_5CH_2)_4C_{60}]^{2-}$ (Figure 9) also shows a small absorption at 1372 nm which is most likely not related to the 1374 nm band of $[(C_6H_5CH_2)_4C_{60}]^-$. Indeed, the 1372 nm band does not increase significantly in magnitude with the time of the measurement, thus ruling out the possibility that $[(C_6H_5CH_2)_4C_{60}]^{2-}$ decomposes to $[(C_6H_5CH_2)_4C_{60}]^-$ during the time of the spectral measurement. A blue-shift of the characteristic absorption bands is also observed upon going from $[(C_6H_5CH_2)_4C_{60}]^-$ to $[(C_6H_5CH_2)_4C_{60}]^{2-}$.

As seen in Table 6, the C_{60}^- and C_{60}^{2-} anions are characterized by only one major near-IR band, while two major bands are seen for the derivatized monoanions ($R_2C_{60}^-$ and $R_4C_{60}^-$) and dianions ($R_2C_{60}^{2-}$ and $R_4C_{60}^{2-}$). One of the two near-IR bands of the derivative is red-shifted with respect to the near-IR band of C_{60}^- or C_{60}^{2-}, while the other is blue-shifted. Such a change in the near-IR spectra of the derivatized anions may be ascribed to a splitting of the triply degenerate t_{1u} and t_{1g} orbitals of C_{60}, caused by a reduction in symmetry in R_2C_{60} and R_4C_{60}. A splitting of the degeneracy may also result in smaller molar absorptivities for the near-IR bands of anionic R_2C_{60} or R_4C_{60} as compared to those of the corresponding anions of C_{60}. It should be pointed out, however, that the energy difference (given as ΔE in eV) between the near-IR absorptions labeled as band I in $[R_2C_{60}]^-$ and $[R_2C_{60}]^{2-}$ or band II in the mono- and dianionic forms of the same derivative are similar to one another (0.12 and 0.13 eV) and close to the ΔE value observed for C_{60} (0.15 eV) and R_4C_{60} (0.11 and 0.14 eV).

Conclusion

R_2C_{60} where R = $C_6H_5CH_2$, 2-$BrC_6H_4CH_2$, 3-$BrC_6H_4CH_2$, and 4-$BrC_6H_4CH_2$ and R_4C_{60} where R = $C_6H_5CH_2$ were prepared by electrosynthetic methods and characterized as to their electrochemical and spectral properties. UV−visible and NMR data show that the R_2C_{60} derivatives are 1,4-adducts of C_{60}, while mass spectral and NMR results confirm the formation of R_4C_{60}. All of the investigated mono- and dianionic R_2C_{60} and R_4C_{60} species display two well-defined near-IR marker bands, one of which is red-shifted and the other blue-shifted with respect to the characteristic absorption band of mono- and dianionic C_{60}.

The electrochemistry shows that the half-wave potential for the third reduction of $(C_6H_5CH_2)_4C_{60}$ in PhCN containing 0.1 M TBAP is shifted negatively by 550 mV with respect to the third reduction of C_{60} under the same experimental conditions. This difference is much larger than the potential difference between the first or second reductions of the same two compounds and can be accounted for by a significant split of the degeneracy in the triply degenerate t_{1u} orbitals of C_{60} in R_4C_{60} which has no symmetry as compared with R_2C_{60}.

Acknowledgment. We thank the Robert A. Welch Foundation (K.M.K., Grant E-680), the Petroleum Research Fund (K.M.K., Grant ACS-PRF 27598-AC5), and an International Scientific Research Program (08044083) from the Ministry of Education, Science, Culture and Sport, Japan for financial support.

References and Notes

(1) Haufler, R. E.; Conceicao, J.; Chibante, L. P. F.; Chai, Y.; Byrne, N. E.; Flanagan, S.; Haley, M. M.; O'Brien, S. C.; Pan, C.; Xiao, Z.; Billups, W. E.; Ciufolini, M. A.; Hauge, R. H.; Margrave, J. L.; Wilson, L. J.; Curl, R. F.; Smalley, R. E. *J. Phys. Chem.* **1990**, *94*, 8634.

(2) Allemand, P.-M.; Koch, A.; Wudl, F.; Rubin, Y.; Diederich, F.; Alvarez, M. M.; Anz, S. J.; Whetten, R. L. *J. Am. Chem. Soc.* **1991,** *113*, 1050.

(3) Dubois, D.; Kadish, K. M.; Flanagan, S.; Haufler, R. E.; Chibante, L. P. F. Wilson, L. J. *J. Am. Chem. Soc.* **1991,** *113*, 4364.

(4) Dubois, D.; Kadish, K. M.; Flanagan, S.; Wilson, L. J. *J. Am. Chem. Soc.* **1991,** *113*, 7773.

(5) Xie, Q.; Pérez-Cordero, E.; Echegoyen, L. *J. Am. Chem. Soc.* **1992,** *114*, 3978.

(6) Krätschmer, W.; Lamb, L. D.; Fostiropoulos, K.; Huffman, D. R. *Nature* **1990**, *347*, 354.

(7) Suzuki, T.; Li, Q.; Khemani, K. C.; Wudl, F.; Almarsson, Ö. *Science* **1991**, *254*, 1186.

(8) Wudl, F. *Acc. Chem. Res.* **1992**, *25*, 157.

(9) Bingel, C. *Chem. Ber.* **1993**, *126*, 1957.

(10) Hirsch, A.; Soi, A.; Karfunkel, H. R. *Angew. Chem., Int. Ed. Engl.* **1992**, *31*, 766.

(11) Caron, C.; Subramanian, R.; D'Souza, F.; Kim, J.; Kutner, W.; Jones, M. T.; Kadish, K. M. *J. Am. Chem. Soc.* **1993**, *115*, 8505.

(12) Subramanian, R.; Kadish, K. M.; Vijayashree, M. N.; Gao, X.; Jones, M. T.; Miller, M. D.; Krause, K. L.; Suenobu, T.; Fukuzumi, S. *J. Phys. Chem.* **1996**, *100*, 16327.

(13) Chen, J.; Cai, R.-F.; Huang, Z.-E.; Wu, H.-M.; Jiang, S.-K.; Shao, Q.-F. *J. Chem. Soc., Chem. Commun.* **1995**, 1553.

(14) Boulas, P. L.; Zuo, Y.; Echegoyen, L. *Chem. Commun.* **1996**, 1547.

(15) Mangold, K.-M.; Kutner, W.; Fröhner, D. J. *Synth. Met.* **1996**, *77*, 73.

(16) Diederich, F.; Thilgen, C. *Science* **1996**, *271*, 317−323.

(17) Diederich, F.; Isaacs, L.; Philip, D. *Chem. Soc. Rev.* **1994**, 243−255.

(18) Taylor, R.; Walton, D. R. M. *Nature* **1993**, *363*, 685−693.

(19) Lerke, S. A.; Parkinson, B. A.; Evans, D. H.; Fagan, P. J. *J. Am. Chem. Soc.* **1992**, *114*, 7807.

(20) Evans, D. H.; Lerke, S. A. *Recent Advances in the Chemistry and Physics of Fullerene and Related Materials*; Kadish, K. M., Ruoff, R. S., Eds.; The Electrochemical Society: Pennington, NJ, 1994; Vol. 1, p 1087.

(21) Kadish, K. M.; Boulas, P. L.; Vijayashree, M. N.; Subramanian, R.; Gao, X.; Mead, S.; Tan, Z.; Jones, M. T. *Recent Advances in the Chemistry and Physics of Fullerene and Related Materials*; Ruoff, R. S., Kadish, K. M., Eds.; The Electrochemical Society: Pennington, NJ, 1995; Vol. 2, p 213.

(22) Arias, F.; Echegoyen L.; Wilson, S. R.; Lu, Q.; Lu, Q. *J. Am. Chem. Soc.* **1995**, *117*, 1422.

(23) Boulas, P.; D'Souza, F.; Henderson, C. C.; Cahill, P. A.; Jones, M. T.; Kadish, K. M. *J. Phys. Chem.* **1993**, *97*, 13435.

(24) Balch, A. L.; Cullison, B.; Fawcett, W. R.; Ginwalla, A. S.; Olmstead, M. M. Winkler, K. *J. Chem. Soc., Chem. Commun.* **1995**, 2287.

(25) Paolucci, F.; Marcaccio, M.; Roffia, S.; Orlandi, G.; Zerbetto, F.; Prato, M.; Maggini, M.; Scorrano, G. *J. Am. Chem. Soc.* **1995**, *117*, 6572.

(26) Llacay, J.; Mas, M.; Molins, E.; Veciana, J.; Powell, D.; Rovira, C. *Chem. Commun.* **1997**, 659.

(27) Nagashima, H.; Saito, M.; Kato, Y.; Goto, H.; Osawa, E.; Haga, M.; Itoh, K. *Tetrahedron* **1996**, *52*, 5053.

(28) Suzuki, T.; Maruyama, Y.; Akasaka, T.; Ando, W.; Kobayashi, K.; Nagase, S. *J. Am. Chem. Soc.* **1994,** *116*, 1359.

(29) Zhou, J.; Rieker, A.; Grösser, T.; Skiebe, A.; Hirsch, A. *J. Chem. Soc., Perkin Trans. 2* **1997**, 1.

(30) Eiermann, M.; Haddon, R. C.; Knight, B.; Li. Q. C.; Maggini, M.; Martin, N.; Ohno, T.; Prato, M.; Suzuki T.; Wudl, F. *Angew. Chem., Int. Ed. Engl.* **1995**, *34*, 1591.

(31) Keshavarz-K. M.; Knight, B.; Haddon, R. C.; Wudl, F. *Tetrahedron* **1996**, *52*, 5149.

(32) Wang, G.-W.; Komatsu, K.; Murata, Y.; Shiro, M. *Nature* **1997**, *387*, 583.

(33) Baumgarten, M.; Gherghel, L. *Appl. Magn. Reson.* **1996**, *11*, 171.

(34) Lawson, D. R.; Feldheim, D. L.; Foss, C. A.; Dorhout, P. K.; Elliott, C. M.; Martin, C. R.; Parkinson, B. *J. Electrochem. Soc.* **1992**, *139*, L68.

(35) Greaney, M. A.; Gorun, S. M. *J. Phys. Chem.* **1991**, *95*, 7142.

(36) Ohlendorf, V.; Willnow, A.; Hungerbühler, H.; Guldi, D. M.; Asmus, K.-D. *J. Chem. Soc., Chem. Commun.* **1995**, 759.

(37) Stinchcombe, J.; Pénicaud, A.; Bhyrappa, P.; Boyd, P. D. W.; Reed, C. A. *J. Am. Chem. Soc.* **1993**, *115*, 5212.

(38) Boyd, P. D. W.; Bhyrappa, P.; Paul, P.; Stinchcombe, J.; Bolskar, R. D.; Sun, Y.; Reed, C. A. *J. Am. Chem. Soc.* **1995**, *117*, 2907.

(39) Subramanian, R.; Boulas, P.; Vijayashree, M. N.; D'Souza, F.; Jones, M. T.; Kadish, K. M. *J. Chem. Soc., Chem. Commun.* **1994**, 1847.

(40) Trulove, P. C.; Carlin, R. T.; Eaton, G. R.; Eaton, S. S. *J. Am. Chem. Soc.* **1995**, *117*, 6265.

(41) Khaled, M. M.; Carlin, R. T.; Trulove, P. C.; Eaton, G. R.; Eaton, S. S. *J. Am. Chem. Soc.* **1994**, *116*, 3465.

(42) Birkett, P. R.; Avent, A. G.; Darwish, A. D.; Kroto, H. W.; Taylor, R.; Walton, D. R. M. *J. Chem. Soc., Perkin Trans. 2* **1997**, 457.

(43) Komatsu, K.; Murata, Y. *Recent Advances in the Chemistry and Physics of Fullerenes and Related Materials;* Kadish, K. M., Ruoff, R. S., Eds.; The Electrochemical Society: Pennington, NJ, 1997; Vol. 4, p 199.

(44) Sawamura, M.; Iikura, H.; Nakamura, E. *J. Am. Chem. Soc.* **1996**, *118*, 12850.

(45) Stewart, J. J. P. *J. Comput. Chem.* **1989**, *10*, 209, 221.

(46) Ajie, H.; Alvarez, M. M.; Anz, S. J.; Beck, R. D.; Diederich, F.; Fostiropoulos, K.; Huffman, D. R.; Krätschmer, W.; Rubin, Y.; Schriver, K. E.; Sensharma, D.; Whetten, R. L. *J. Phys. Chem.* **1990**, *94*, 8630.

(47) Hare, J. P.; Kroto, H. W.; Taylor, R. *Chem. Phys. Lett.* **1991**, *177*, 394.

(48) Smith, A. B., III; Strongin, R. M.; Brard, L.; Furst, G. T.; Romanow, W. J.; Owens, K. G.; Goldschmidt, R. J.; King, R. C. *J. Am. Chem. Soc.* **1995**, *117*, 5492.

(49) D'Souza, F.; Caron, C.; Subramamian, R.; Kutner, W.; Jones, M. T.; Kadish, K. M. *Recent Advances in the Chemistry and Physics of Fullerene and Related Materials*; Kadish, K. M., Ruoff, R. S., Eds.; The Electrochemical Society: Pennington, NJ, 1994; Vol. 1, p 768.

(50) Miki, S.; Kitao, M.; Fukunishi, K. *Tetrahedron Lett.* **1996**, *37*, 2049.

(51) Komatsu, K.; Murata, Y.; Wang, G.-W.; Wan, T. S. M. *Recent Advances in the Chemistry and Physics of Fullerene and Related Materials*; Kadish, K. M., Ruoff, R. S., Eds.; The Electrochemical Society: Pennington, NJ, 1996; Vol. 3, p 1200.

(52) Sanders, J. K. M.; Hunter, B. K. *Modern NMR Spectroscopy*; Oxford University Press: Oxford, 1986; pp 299−302.

(53) Richards, S. A. *Laboratory Guide to Proton NMR Spectroscopy*; Blackwell Scientific Publications: Oxford, 1988; pp 82−92.

(54) Pouchert, C. J.; Behnke, J. *The Aldrich Library of ^{13}C and ^{1}H FT NMR Spectra*; 1st ed.; Aldrich Chemical Co., Inc.: Milwaukee, WI, 1993; Vol. 2.

(55) Whitesides, G. M.; Holtz, D.; Roberts, J. D. *J. Am. Chem. Soc.* **1964**, *86*, 2628.

(56) Whitesides, G. M.; Grocki, J. J.; Holtz, D.; Steinberg, H.; Roberts, J. D. *J. Am. Chem. Soc.* **1965**, *87*, 1058.

(57) Our preliminary computer simulation results indicate that there is a much higher energy barrier for the rotation of phenyl groups of $(2\text{-BrC}_6\text{H}_4\text{CH}_2)_2\text{C}_{60}$ than those for the rotation of phenyl groups of the other three compounds, thus, suggesting that the phenyl groups in $(2\text{-BrC}_6\text{H}_4\text{CH}_2)_2\text{C}_{60}$ would be favored in assuming a conformation similar to that shown in Chart 1a, which consequently would result in a large $\Delta\delta$ value.

(58) Marcus, R. A. *Annu. Rev. Phys. Chem.* **1964**, *15*, 155.

(59) The calculation was performed for the following $(\text{C}_6\text{H}_5\text{CH}_2)_4\text{C}_{60}$ isomer which has C_1 symmetry: 1, 4, 16, 36-$(\text{C}_6\text{H}_5\text{CH}_2)_4\text{C}_{60}$.